European Heart Journal – Cardiovascular Imaging (2015) **16**, 166–176
doi:10.1093/ehjci/jeu217

Relationship of left ventricular mass to coronary atherosclerosis and myocardial ischaemia: the CORE320 multicenter study

Satoru Kishi[1], Tiago A. Magalhaes[1], Richard T. George[1], Marc Dewey[2], Roger J. Laham[3], Hiroyuki Niinuma[4], Lisa Aronson Friedman[5], Christopher Cox[5], Yutaka Tanami[6], Joanne D. Schuijf[7], Andrea L. Vavere[1], Kakuya Kitagawa[8], Marcus Y. Chen[9], Cesar H. Nomura[10], Jeffrey A. Brinker[1], Frank J. Rybicki[11], Marcelo F. Di Carli[11], Armin Arbab-Zadeh[1], and Joao A.C. Lima[1]*

[1]Division of Cardiology, Department of Medicine, Johns Hopkins University School of Medicine, Blalock 524, 600 N. Wolfe Street, Baltimore, MD 21287, USA; [2]Department of Radiology, Charité Medical School, Humboldt-Universität zu Berline and Freie Universität zu Berlin, Berlin, Germany; [3]Division of Cardiology, Beth Israel Deaconess Medical Center, Boston, MA, USA; [4]Division of Cardiology, St. Luke's International Hospital, Tokyo, Japan; [5]Johns Hopkins Bloomberg School of Public Health, Baltimore, MD, USA; [6]Department of Radiology, Keio University, Tokyo, Japan; [7]Toshiba Medical Systems Europe B.V., Zoetermeer, The Netherlands; [8]Department of Radiology, Mie University Hospital, Tsu, Japan; [9]Advanced Cardiovascular Imaging Group, National Heart, Lung, and Blood Institute, National Institutes of Health, Bethesda, MD, USA; [10]Radiology Sector, Hospital Israelita Albert Einstein, São Paulo, Brazil; and [11]Department of Radiology, Brigham and Women's Hospital, Harvard University, Boston, MA, USA

Received 6 April 2014; accepted after revision 12 September 2014; online publish-ahead-of-print 3 November 2014

Aims The aim of this study was to investigate the association of left ventricular mass (LVM) with coronary atherosclerosis and myocardial infarction (MI).

Methods and results Patients ($n = 338$) underwent 320 × 0.5 mm detector row coronary computed tomography (CT) angiography, invasive coronary angiography (ICA), and single-photon emission CT (SPECT) myocardial perfusion imaging. Quantitative coronary atheroma volume was obtained from the CT images for the entire coronary tree (19-segment model) with an arterial contour detection algorithm. Normalized total atheroma volume (NormTAV) was analysed to reflect quantitative total atheroma volume. LVM was measured on myocardial CT images and indexed to height to the power of 2.7 (LVMi). Patients with obstructive coronary artery disease (CAD) were defined as those with ≥50% diameter stenosis by quantitative ICA. Abnormal perfusion defect was defined as ≥1 abnormal myocardial segment by SPECT. The association of LVMi with coronary atherosclerosis and myocardial perfusion defect on SPECT at the patient level was determined with uni- and multivariable linear and logistic regression analyses. Obstructive CAD was present in 60.0% of enrolled patients. LVMi was independently associated with abnormal summed rest score [SRS; odds ratio (OR), 1.07; 95% confidence interval (CI), 1.03–1.09] and summed stress score (OR, 1.04; 95% CI, 1.01–1.07). An increase in LVMi was also independently associated with that in NormTAV (coefficient, 10.44; 95% CI, 1.50–19.39) and SRS ≥1 (OR, 1.05; 95% CI, 1.01–1.10), even after adjusting for cardiovascular risk factors in patients without previous MI.

Conclusions LVM was independently associated with the presence of coronary artery atherosclerosis and MI.

Keywords Coronary atherosclerosis • Left ventricular mass • Myocardial ischaemia • Atheroma volume

Introduction

Increased left ventricular mass (LVM) is an independent predictor of cardiovascular morbidity and mortality.[1,2] The Framingham study showed that a 50% increase in LVM determined by echocardiography independently predicts coronary heart disease (CHD) in both men and women.[3] Increased LVM is also related to coronary artery disease (CAD).[4,5]

* Corresponding author. Tel: +1 410 614 1284; Fax: +1 410 287 6625, Email: jlima@jhmi.edu

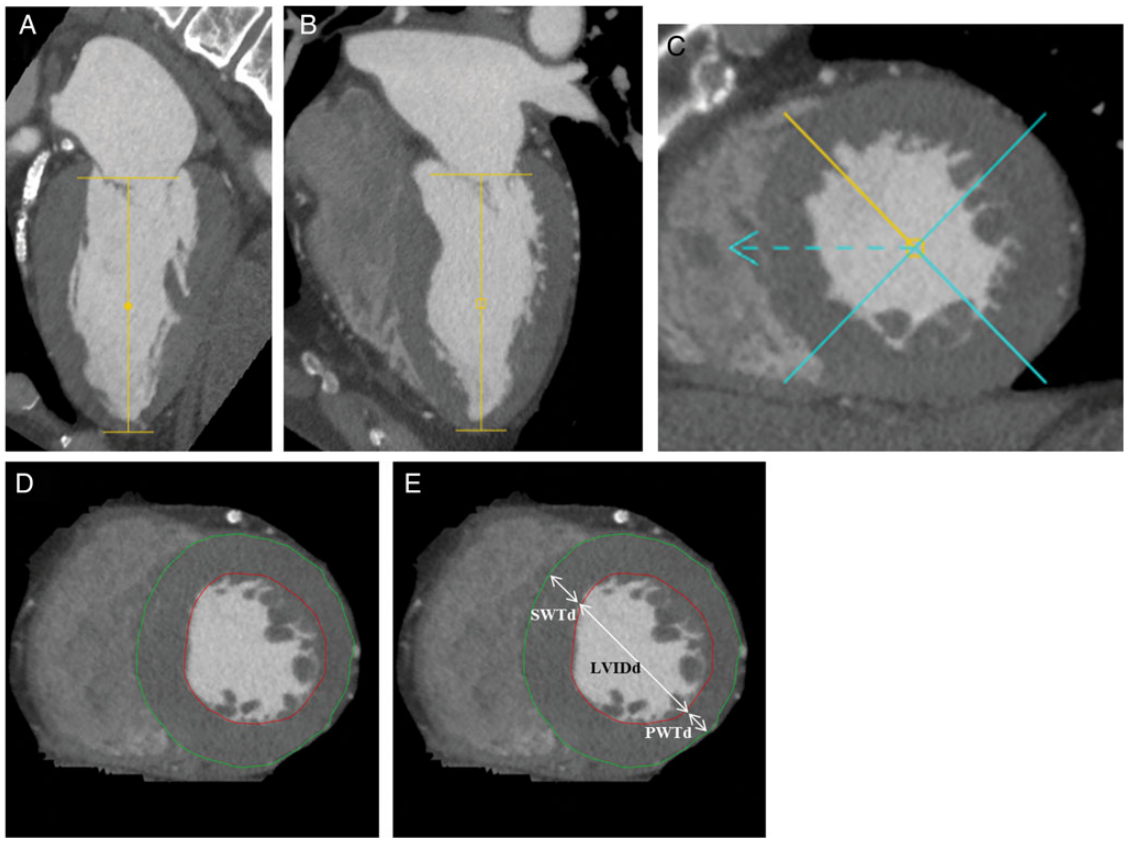

Figure 1: Method of LV structure. (*A–C*) The software displays the segmented LV in short-axis view and two long-axis views. (*D*) The software displays the segmented LV in short-axis view with automatic tracing of endo- and epicardial contours. The software could manually adjust the mitral valve plane, apex plane, LV axis, and endo- and epicardial contours. The papillary muscles and trabeculae were regarded as part of the LV cavity. (*E*) Endo-diastolic wall thicknesses [anteroseptal (SWTd) and posterior (PWTd)] and LV internal diameter (LVIDd) on short-axis planes were measured as the LV mid-papillary level.

Multidetector computed tomography (CT), with improved temporal and spatial resolution, enables single heart beat evaluation of coronary atherosclerosis and cardiac structure.[6,7] A meta-analysis found excellent agreement between CT and cardiovascular magnetic resonance imaging for global LV function.[8] A previous study using CT suggested that LVM is associated with the degree of coronary plaque burden.[9] Although single-photon emission CT (SPECT) indicates that LVM is associated with myocardial ischemia, the relationship of LVM with quantified total coronary atheroma volume and myocardial infarction (MI) is unknown.[10] The purpose of this study is to test the hypothesis that LVM measured with CT is associated with coronary atherosclerosis and MI.

Methods

CORE320 study design and study population

The study design of the CORE320 is a prospective, multicentre, multinational, and diagnostic study designed to detect patients with atherosclerosis and corresponding myocardial ischemia.[11,12] The study was designed to compare the accuracy of combined CT coronary angiography (CTA) and myocardial CT perfusion imaging against the combination of reference standard invasive coronary angiography (ICA) and SPECT myocardial perfusion imaging, and includes patients 45–85 years of age who were referred for clinically indicated ICA for suspected or known CAD within a 60-day period and who are willing and able to provide written informed consent.[11] Of 381 patients who were enrolled in CORE320, patients with $<80\%$ of the cardiac phase ($n = 22$) were excluded because LVM and LV end-diastolic volume (LVEDV) could not be evaluated in the absence of end-diastolic phase. In addition, 21 patients had non-diagnostic image quality. The remaining 338 participants were included in this study.

CT acquisition and analysis

Detailed descriptions of the CORE320 CT image acquisition and interpretation methods have been published previously.[12,13]

Coronary atheroma volume analysis

All reconstructed datasets were transferred to an offline workstation to perform quantitative coronary atheroma volume analysis using the dedicated software with a semi-automated 3D contour detection algorithm (QAngio CT Research Edition version 2.0 RC4, Medis Medical Imaging Systems, Leiden, The Netherlands).[14,15] In addition to quantitative

Table 1 Participant characteristics

Variables	All $n = 338$	Obstructive CAD $n = 203$ (60.0%)	Non-obstructive CAD $n = 135$ (40.0%)	*P*-value
Age, in years*	62.0 (55.7–68.4)	63.1 (56.2–69.4)	61.0 (54.5–67.3)	0.03
Male*	228 (67)	162 (80)	66 (49)	<0.0001
Asian	110 (33)	75 (37)	35 (26)	0.05
African-American	38 (11)	18 (9)	20 (15)	
Caucasian	190 (56)	109 (54)	80 (59)	
BMI*, kg/m^2	26.6 (24.1–30.2)	26.2 (24.0–29.3)	27.3 (24.2–31.6)	0.03
Waist circumference	91.0 (83.5–100.0)	90.5 (83.5–99.0)	91.0 (83.5–101.0)	0.30
Hypertension*	264 (79)	167 (83)	97 (72)	0.03
Diabetes	119 (35)	78 (38)	41 (30)	0.13
Dyslipidaemia*	220 (67)	147 (74)	73 (55)	0.0005
Previous MI*	84 (26)	73 (36)	19 (14)	<0.0001
Smoking				
Current	56 (17)	30 (16)	26 (20)	0.05
Past	116 (36)	79 (41)	37 (28)	
Never	150 (47)	82 (43)	68 (52)	
Family history of CAD	147 (46)	91 (48)	56 (43)	0.36
Calcium score, Agatston score	154 (11–502)	342 (112–800)	11 (0–118)	<0.0001
LVIDd, mm	49.8 (46.2–53.8)	49.8 (46.2–54.3)	49.9 (46.1–53.6)	0.87
PWTd*, mm	9.2 (8.1–10.2)	9.4 (8.3–10.5)	8.9 (8.0–9.7)	0.009
LVEDV, mL	105 (90–123)	107 (90–126)	104 (92–122)	0.39
LVM*, g	148 (128–174)	152 (130–181)	145 (123–161)	0.008
LVMi (height$^{2.7}$), g/m$^{2.7}$	36.7 (32.7–43.2)	37.8 (33.0–44.7)	36.0 (32.0–40.5)	0.07
LVM/LVEDV ratio	1.36 (1.18–1.62)	1.39 (1.21–1.66)	1.32 (1.15–1.56)	0.11
RWT*	0.36 (0.32–0.42)	0.37 (0.33–0.43)	0.35 (0.32–0.40)	0.04
Concentric hypertrophy	8 (2)	6 (3)	2 (1)	0.09
Eccentric hypertrophy	23 (7)	14 (7)	9 (7)	
Concentric remodelling	68 (20)	49 (24)	19 (14)	
Normal geometry	239 (71)	134 (66)	105 (78)	
PAV*, %	54.1 (49.6–59.0)	57.3 (54.1–60.9)	49.5 (46.4–52.7)	<0.0001
NormTAV*, mm^3	2845 (2414–3178)	2996 (2681–3354)	2476 (2210–2914)	<0.0001
SPECT: SRS ≥1*	122 (36)	93 (46)	29 (21)	<0.0001
SPECT: SSS ≥1*	172 (51)	124 (61)	48 (36)	<0.0001
SPECT: SDS ≥1*	136 (40)	99 (49)	37 (27)	0.0001

Values are median (IQR) or *n* (%). Waist circumference data missing for 127 (63%) subjects with obstructive CAD and 79 (59%) subjects with non-obstructive CAD. *P*-values from the Wilcoxon rank-sum test (continuous variables) or Fisher's exact test (categorical variables).
BMI, body mass index; CAD, coronary artery disease; LVEDV, left ventricular end-diastolic volume; LVIDd, left ventricular internal diameter at end-diastole; LVM, left ventricular mass; LVMi, left ventricular mass index; PWTd, posterior wall thickness at end-diastole; RWT, relative wall thickness; SRS, summed rest score; SSS, summed stress score; SDS, summed difference score; PAV, percent atheroma volume; SPECT, single-photon emission computed tomography; NormTAV, normalized total atheroma volume; IQR, interquartile range.
*$P < 0.05$ for difference between the obstructive CAD and non-obstructive CAD groups by the Wilcoxon rank-sum test (continuous measures) or Fisher's exact test (categorical measures).

CTA stenosis assessment, the quantitative atheroma analysis was performed by two independent, experienced observers who were blinded to both quantitative coronary analysis (QCA) and clinical data. The methods of quantitative atheroma analysis using the dedicated atheroma analysis software are described elsewhere.[14,16] The atheroma volume was calculated by subtracting lumen volume from vessel volume for the entire coronary tree using a 19-segment model.[17] For each patient, the vessel volume, lumen volume, atheroma volume, and vessel length were calculated by adding all analysed segments (see Supplementary data online, *Figure S1*). We defined two different quantified total atheroma volume indices.[16]

(i) *Percent atheroma volume (PAV, %)*: (total atheroma volume/total vessel volume) × 100.
(ii) *Normalized total atheroma volume (NormTAV, mm^3)*: (total atheroma volume/segment length) × mean total vessel length, where mean total vessel length = average length of all vessels in the sample.

LV mass

CT sinograms were reconstructed to generate 0.5 mm slice thickness and 0.5 mm in-slice resolution images, using a myocardial perfusion kernel FC03. Images targeting a cardiac phase of 85% of the R–R interval

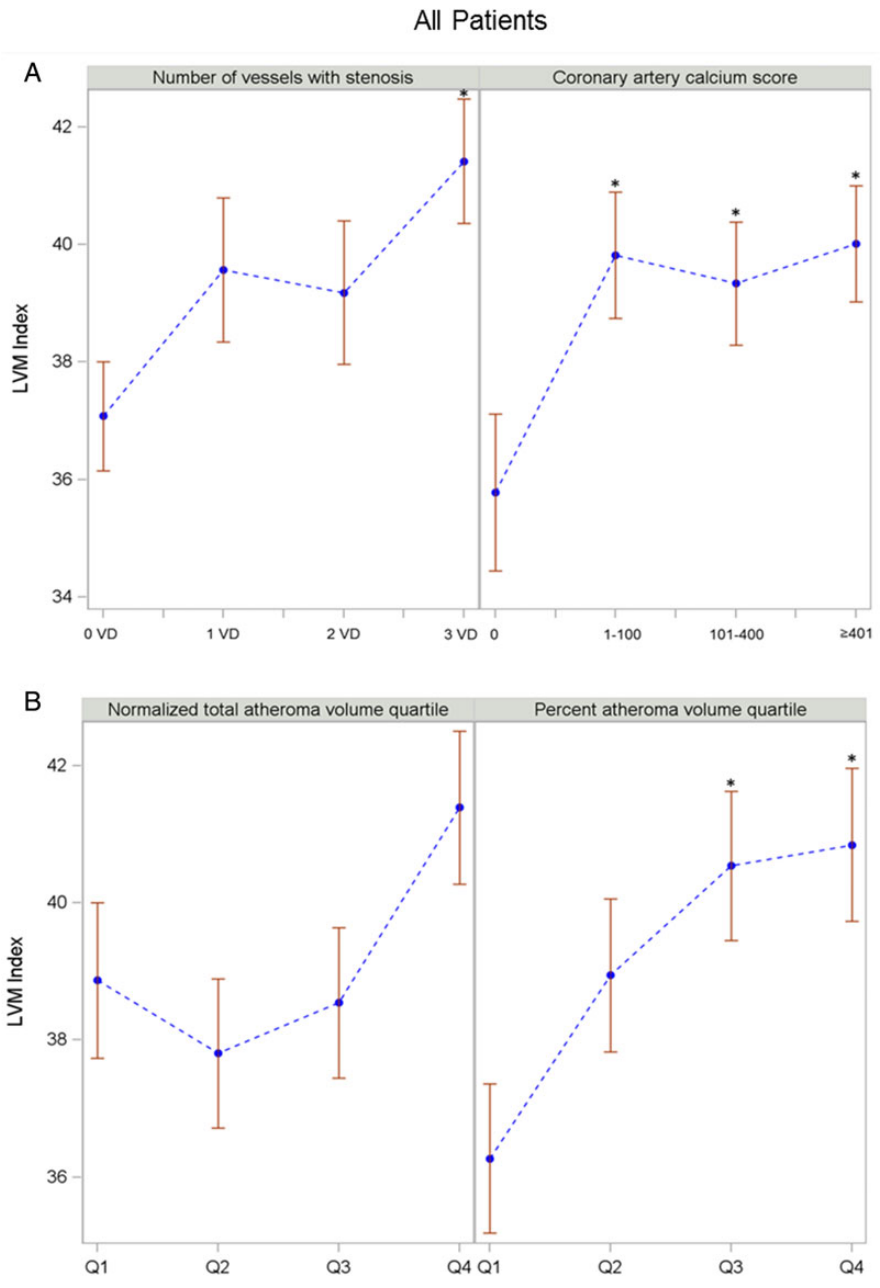

Figure 2: The relationship of LVMi to coronary atherosclerosis in all patients. *$P < 0.05$. Error bars represent standard error. Comparisons by ANOVA. For CTA parameters and atheroma volume indices, vs. no diseased vessel, zero calcium score, and first quartile group as a reference. LVMi (*A*) across CTA parameters: number of vessel disease and categorized coronary calcium score. LVMi (*B*) across atheroma volume indices: NormTAV and PAV.

and a phase window width of 20% were reconstructed at 1% R–R interval spacing for all available phases.[13] The post-processing software (Vitrea FX version 3.0, Vital Images, Minnetonka, MN, USA) displays the segmented LV in short-axis view and two long-axis views with automatic tracing of endo- and epicardial contours. The software allows manual adjustment of the mitral valve plane, apex plane, LV axis, and endo- and epicardial contours (*Figure 1*). The papillary muscles and trabeculae are included as part of the LV cavity. Finally, the end-diastolic phase was determined manually by assessing the largest volume. LVM was calculated as a product of myocardial volume and the specific gravity of the myocardium (1.05 g/cm^3). LVM was indexed to height to the power of 2.7 (LVMi: LVM/height$^{2.7}$).[4] End-diastolic wall thicknesses and LV internal diameter on short-axis planes were measured as the LV mid-papillary level (*Figure 1*). LVEDV was calculated at the end-diastolic phase using Simpson's method.[4] LV geometry was classified according to the American Society of Echocardiography.[4]

Table 2 Relationship of LVMi with coronary atherosclerosis and the presence of MPD by SPECT

Dependent variables	Unadjusted OR (95% CI)	Model 1 OR (95% CI)[a]	Model 2 OR (95% CI)[b]	Model 3 OR (95% CI)[c]
Obstructive CAD	1.01 (0.990–1.04)	1.01 (0.985–1.04)	1.005 (0.977–1.03)	–
Presence of MPD: SRS ≥1	1.05 (1.02–1.07)[‡]	1.06 (1.03–1.09)[‡]	1.06 (1.03–1.09)[‡]	1.07 (1.03–1.10)[‡]
Presence of MPD: SSS ≥1	1.04 (1.01–1.06)[†]	1.04 (1.01–1.07)[†]	1.04 (1.01–1.07)[*]	1.04 (1.01–1.07)[†]
Presence of MPD: SDS ≥1	1.02 (0.996–1.04)	1.01 (0.987–1.04)	1.009 (0.983–1.03)	1.008 (0.982–1.03)
	Beta (95% CI)	Beta (95% CI)[a]	Beta (95% CI)[b]	Beta (95% CI)[c]
Normalized total atheroma volume	10.51 (3.82 to 17.19)[†]	7.72 (−0.07 to 15.51)	5.63 (−0.47 to 11.72)	–
Percent atheroma volume	0.06 (−0.01 to 0.13)	0.05 (−0.04 to 0.13)	0.02 (−0.05 to 0.10)	–

LVMi, left ventricular mass index; SPECT, single-photon emission computed tomography; OR, odds ratio; CI, confidence interval; CAD, coronary artery disease; MPD, myocardial perfusion defect; SRS, summed rest score; SSS, summed stress score; SDS, summed difference score.
[a]Model 1 was adjusted for age, sex, race, BMI, hypertension, dyslipidaemia, diabetes, smoking status, and family history of CAD.
[b]Model 2 was adjusted for all variables in Model 1 plus coronary calcium score.
[c]Model 3 for the presence of MPD was adjusted for all variables in Model 2 plus history of previous MI and obstructive CAD.
[*]$P < 0.05$; [†]$P < 0.01$; [‡]$P < 0.001$.

ICA and SPECT acquisition and analysis

The ICA acquisition and interpretation methods have been described in detail previously.[11–13] Obstructive CAD was defined as ≥50% diameter stenosis by QCA.[11–13]

On the SPECT images, myocardial segments were analysed for rest and stress myocardial perfusion abnormalities with severity-scored as follows: 0 = normal, 1 = mild reduction in tracer activity, 2 = moderate reduction in tracer activity, and 3 = severe reduction in tracer activity using a 13-segment model as previously described.[12,13,18] The site qualification procedures of the independent SPECT core laboratory have been previously described.[11,13,18] In the analysis, artefacts did not contribute to the summed stress score (SSS) and therefore an SSS of ≥1 defined an abnormal SPECT study using previous methods of the SPECT laboratory.[19] The summed rest score (SRS) was the sum of all scores on the rest images, the SSS was the sum of all scores on the stress images, and the summed difference score (SDS) was the difference between the SSS and SRS. The presence of a myocardial perfusion defect (MPD) was defined as SSS ≥1, SRS ≥1, or SDS ≥1.

Covariates

Race, gender, age, and smoking status were reported by study participants. Hypertension was defined as systolic blood pressure ≥140 mmHg, diastolic blood pressure ≥90 mmHg, or use of antihypertensive medications. Body mass index (BMI) was calculated as weight (kg) divided by height in meters squared (m^2). Diabetes was defined as a fasting glucose level of ≥126 mg/dL or use of medication for diabetes. Dyslipidaemia was defined as total cholesterol >200 mg/dL, low-density lipoprotein cholesterol ≥130 mg/dL, high-density lipoprotein cholesterol <40 mg/dL for men and <50 mg/dL for women, or use of lipid-lowering medications. History of CAD was defined as having a history of MI, obstructive coronary artery stenosis on a prior angiogram, or prior coronary revascularization. Family history of CAD was defined as having a first-degree relative (age <45 years for men or <55 years for women) with a history of MI, coronary revascularization, or sudden death.

Statistical analysis

Participants' baseline data were summarized by using median and interquartile range for continuous variables and frequency and percent for categorical variables. We categorized the number of vessels with obstructive CAD (0–3 vessel disease), coronary artery calcium scores (CACS; CACS = 0, 1–100, 101–400, and ≥401), and MPD for the SSS, SRS, and SDS (MPD <0.5, 0.5–<4.0, 4.0–<8.0, and ≥8.0) into four groups, respectively. We also categorized PAV and NormTAV into quartiles. Multivariable logistic regression models or multivariable linear regression models assessed the relationship of LVM index with CAD (obstructive CAD: ≥50% diameter stenosis by QCA, PAV, and NormTAV) and the presence of MPD (SSS ≥1, SRS ≥1, and SDS ≥1). These models were analysed in four ways without any covariate adjustment: Model 1 was adjusted for age, sex, race, BMI, hypertension, dyslipidaemia, diabetes, smoking status, and a family history of CAD; Model 2 was adjusted for all covariates in Model 1 plus CACS; and Model 3 for the presence of MPD was adjusted for all variables in Model 2 plus history of previous MI and obstructive CAD. Additionally, we analysed these relationships separately for patients with or without MI, which was defined as fixed MPD on SPECT.

The inter-/intra-observer agreement for LVM was determined for 22 randomly selected patients, in which 2 readers independently measured the data. One reader re-measured the same cases 1 month later after the first measurement for intra-observer variability. The inter-observer agreement for total coronary atheroma volume was determined for 19 randomly selected patients, in which 2 readers independently measured the data of 19 patients. Bland–Altman plots were computed to assess inter-/intra-observer variability. Statistical significance was determined at $P < 0.05$. All analyses were conducted using SAS (version 9.3 for Windows, SAS Institute, Inc., Cary, NC, USA). All statistical analyses were performed by the CORE320 Statistical Core Laboratory at the Johns Hopkins Bloomberg School of Public Health.

Results

Participant demographics

Baseline characteristics for the 338 patients included in the analyses are summarized in *Table 1*. The median LVMi was 36.7 $g/m^{2.7}$, PAV 54.1%, and NormTAV 2845 mm^3. The prevalence of obstructive CAD (≥50% stenosis), SRS ≥1, SSS ≥1, and SDS ≥1 was 60, 36, 51, and 40%, respectively. Patients with CAD were more likely to

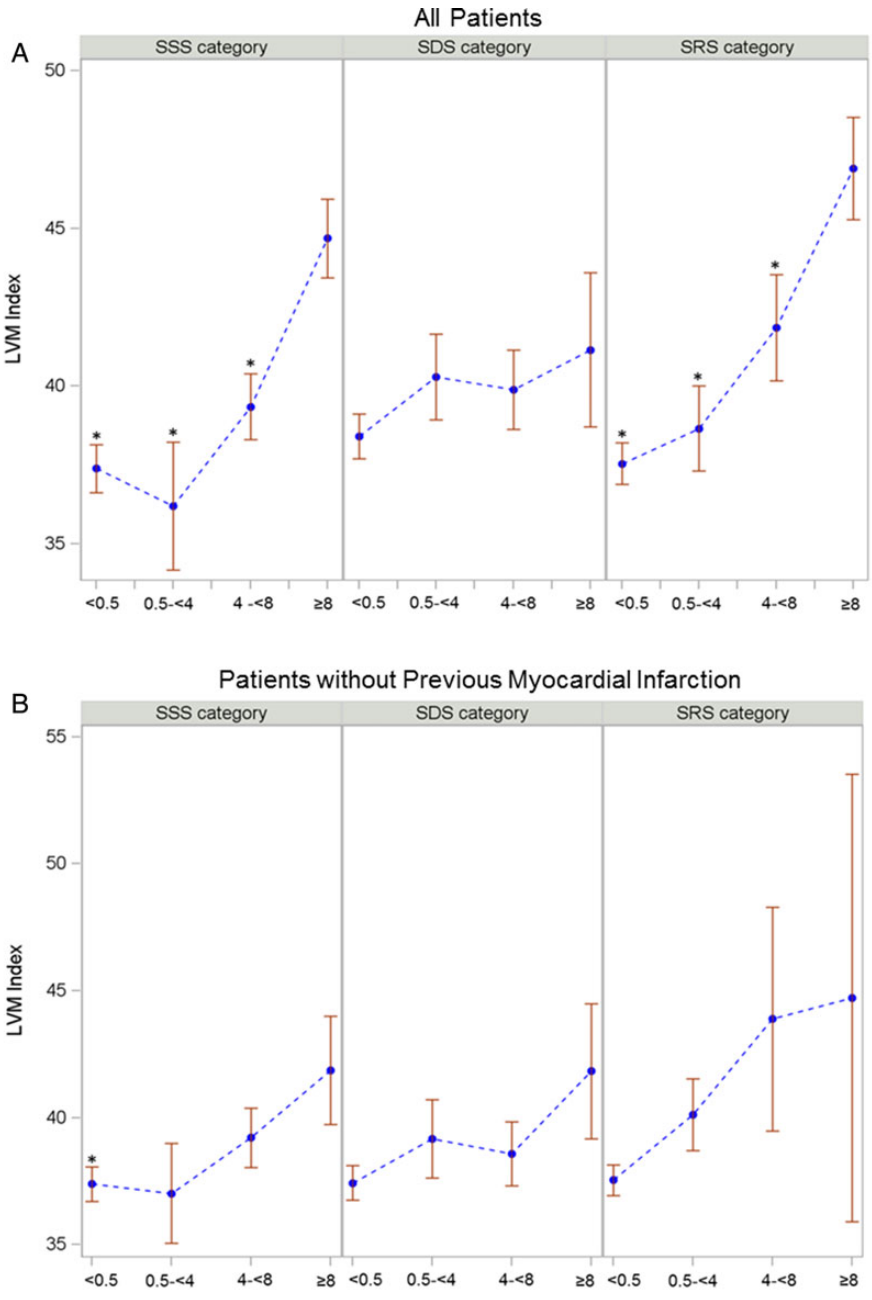

Figure 3: The relationship of LVMi with summed segments of MPD on SPECT. *$P < 0.05$. Error bars represent standard error. Comparisons by ANOVA. For SPECT parameter, vs. SSS, SDS, and SRS ≥ 8 as a reference among categorized summed segments of MPD. LVMi (*A*) across MPD in all patients: categorized SSS, SDS, and SRS. LVMi across MPD among patients without previous MI (*B*).

have concentric remodelling, high PAV and NormTAV, and high SRS, SSS, and SDS ($P < 0.05$ for all).

Relationship of LVM with coronary atherosclerosis and MPDs

Patients with three-vessel disease had a higher LVMi than those with no diseased vessel ($P < 0.05$) (*Figure* 2*A*). Patients in the higher CACS groups had a higher LVMi than those with a zero Agatston score (*Figure* 2*A*). Patients in the third and fourth quartiles of PAV had a higher LVMi than those in the first quartile (*Figure* 2*B*). In univariable linear regression analysis, LVMi was positively associated with NormTAV [β-coefficient, 10.51; 95% confidence interval (CI), 3.82−17.19], but not with obstructive CAD and PAV. However, there was no relationship between LVMi and NormTAV in multivariable analysis (*Table* 2).

Patients with low MPD of SSS and SRS had a lower LVMi compared with those with the highest MPD (*Figure* 3*A*). LVMi was independently

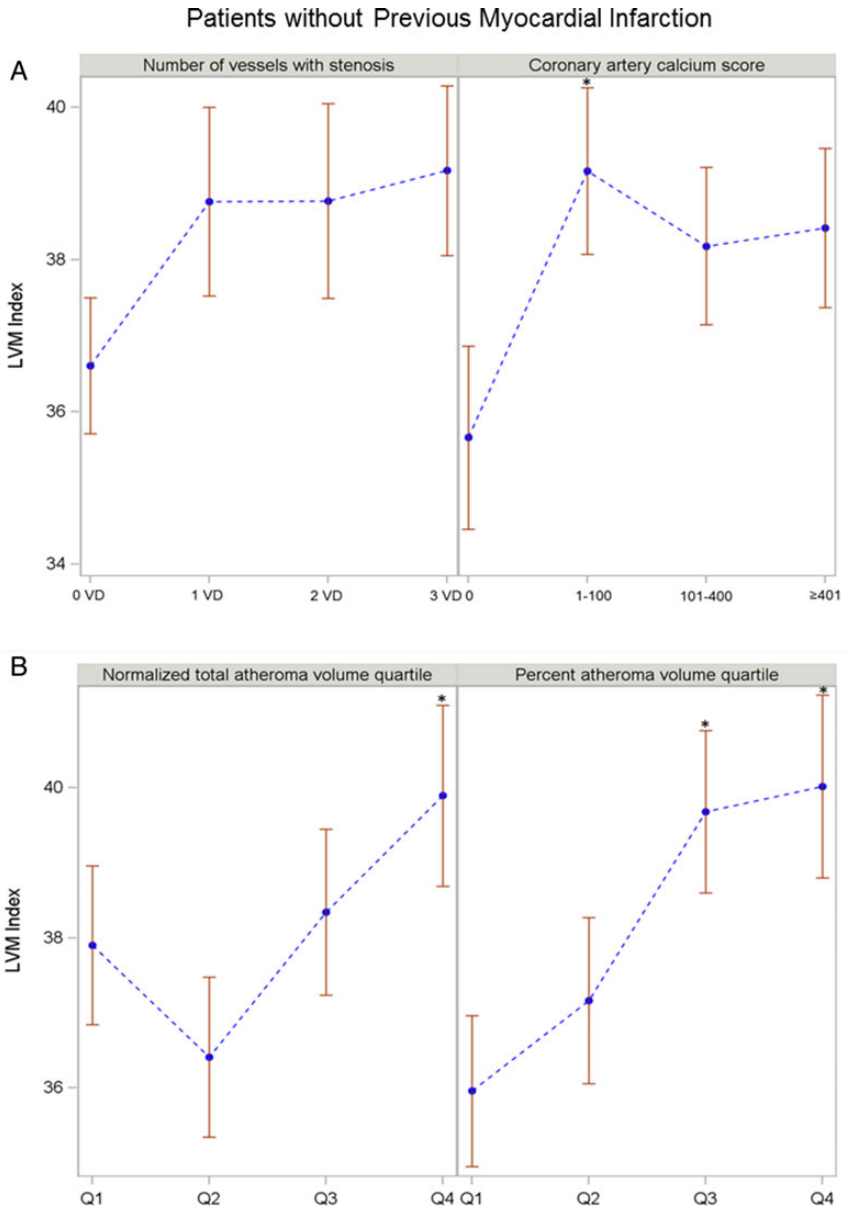

Figure 4: The relationship of LVMi with CTA parameters among patients without previous MI. *$P < 0.05$. Error bars represent standard error. Comparisons by ANOVA. For CTA parameters and atheroma volume indices, vs. no diseased vessel, zero calcium score, and first quartile group as a reference. LVMi (*A*) across CTA parameters: number of vessel disease and categorized coronary calcium score. LVMi (*B*) across atheroma volume indices: NormTAV and PAV.

associated with SRS ≥1 and SSS ≥1 after adjusting for traditional risk factors and obstructive CAD [odds ratio (OR), 1.07; 95% CI, 1.03–1.10 for SRS ≥1; OR, 1.04; 95% CI, 1.01–1.07 for SSS ≥1].

Relationship of LVMi with coronary atherosclerosis and MPDs among patients with and without previous MI

For the 260 patients without previous MI, those in the higher CACS groups had a higher LVMi than those in the zero Agatston score group (*Figure 4A*). Patients in the third and fourth quartiles of PAV had a higher LVMi than those in the first (*Figure 4B*). An increase in LVMi was independently associated with that in NormTAV (β-coefficient, 10.44; 95% CI, 1.50–19.39) even after adjusting for risk factors, but not for PAV (*Table 3*).

In patients without previous MI, a low MPD of SSS had a lower LVMi compared with patients with the highest MPD of SSS (*Figure 3B*). LVMi was independently associated with SRS ≥1 (OR, 1.05; 95% CI, 1.01–1.10) even after adjusting for traditional risk factors and obstructive CAD, but not with SSS ≥1 and SDS ≥1. There was no relationship between LVMi coronary atherosclerosis or SPECT parameters in patients with previous MI (*Table 4*).

Table 3 Multivariate analysis of the relationship of LVMi with coronary atherosclerosis and the presence of MPD by SPECT excluding all patients with MI (fixed defect on SPECT) ($n = 260$)

Dependent variables	Unadjusted OR (95% CI)	Model 1 OR (95% CI)[a]	Model 2 OR (95% CI)[b]	Model 3 OR (95% CI)[c]
Obstructive CAD	1.02 (0.987–1.04)	1.02 (0.983–1.06)	1.01 (0.977–1.05)	–
Presence of MPD: SRS ≥1	1.04 (1.001–1.07)*	1.06 (1.01–1.10)*	1.05 (1.01–1.09)*	1.05 (1.01–1.10)*
Presence of MPD: SSS ≥1	1.02 (0.995–1.05)	1.03 (0.995–1.06)	1.02 (0.987–1.06)	1.02 (0.986–1.06)
Presence of MPD: SDS ≥1	1.02 (0.993–1.05)	1.03 (0.993–1.06)	1.02 (0.986–1.06)	1.02 (0.984–1.05)
	Beta (95% CI)	Beta (95% CI)[a]	Beta (95% CI)[b]	Beta (95% CI)[c]
Normalized total atheroma volume	10.75 (2.12 to 19.39)*	12.85 (1.81 to 23.89)*	10.44 (1.50 to 19.39)*	–
Percent atheroma volume	0.07 (−0.02 to 0.16)	0.07 (−0.04 to 0.19)	0.05 (−0.06 to 0.15)	–

Models and abbreviations are given in Table 2.
*$P < 0.05$.

Table 4 Multivariate analysis of the relationship of LVMi with coronary atherosclerosis and the presence of MPD by SPECT including only patients with MI (fixed defect on SPECT) ($n = 78$)

Dependent variables	Unadjusted OR (95% CI)	Model 1 OR (95% CI)[a]	Model 2 OR (95% CI)[b]	Model 3 OR (95% CI)[c]
Obstructive CAD	0.983 (0.944–1.02)	0.955 (0.899–1.01)	0.953 (0.894–1.02)	–
Presence of MPD: SDS ≥1	0.995 (0.961–1.03)	0.958 (0.909–1.010)	0.955 (0.904–1.008)	1.008 (0.982–1.03)
	Beta (95% CI)	Beta (95% CI)[a]	Beta (95% CI)[b]	Beta (95% CI)[c]
Normalized total atheroma volume	4.62 (−6.47 to 15.70)	−4.28 (−17.4 to 8.81)	−1.85 (−10.5 to 6.78)	–
Percent atheroma volume	−0.02 (−0.13 to 0.09)	−0.06 (−0.22 to 0.09)	−0.04 (−0.18 to 0.09)	–

Models and abbreviations are given in Table 2.
*$P < 0.05$.

Variability of inter- and intra-observer measurements

The inter-observer agreement of LVM was high (bias, −4.66; SD ratio, 1.00; and correlation, 0.99; *Figure 5A*). Intra-observer agreement of LVM was also high (bias, 1.34; SD ratio, 0.99; and correlation, 0.99 for LVM; *Figure 5B*). Inter-observer correlation of total atheroma volume was high ($r = 0.99$).

Discussion

The main finding of this study was that, using CT with a comprehensive reference standard for myocardial ischaemia in the CORE320 population, LVM was related to MI independently of coronary artery atherosclerosis and other risk factors. Furthermore, LVM was positively associated with coronary atheroma volume among patients without previous MI. To our knowledge, our study is the first to report this relationship between LVM and both coronary atherosclerosis and MI.

Relationship of LVM with coronary atherosclerosis

LVM was positively associated with quantified high total coronary atheroma volume in patients without previous MI, but not with previous MI. Similarly, LVMi was associated with calcified plaque and two- or three-vessel disease. A previous study showed a correlation between LV hypertrophy and the number of vessels with CAD.[20] The absolute presence, extent, and severity of non-obstructive CAD have been shown to be associated with LVM among patients without obstructive CAD.[21] Furthermore, LVM and concentric remodelling are associated with a greater degree of coronary atheroma burden in patients without LV hypertrophy.[9] Our findings on the association of coronary atherosclerosis and LVM are consistent with the previously published data.[9,21] Although previous studies used categorized segmental coronary stenosis assessment visually, no prior study has evaluated the relationship between LVM and total atheroma volume quantitatively. An increase in LVMi was independently associated with that in high NormTAV, even after adjusting for cardiovascular risk factors in patients without previous MI. In patients with previous MI, nevertheless, there was no relationship between LVMi and total coronary atheroma volume. LVM is also a consequence of a mix of several confounding risk factors such as hypertension, dyslipidaemia, obesity, smoking status, gender, and aging.[1,2,22] The CORE320 population has multiple atherosclerotic risk factors that may attenuate the relationship between LVM and coronary atherosclerosis, especially among those patients with previous MI (*Table 1*).

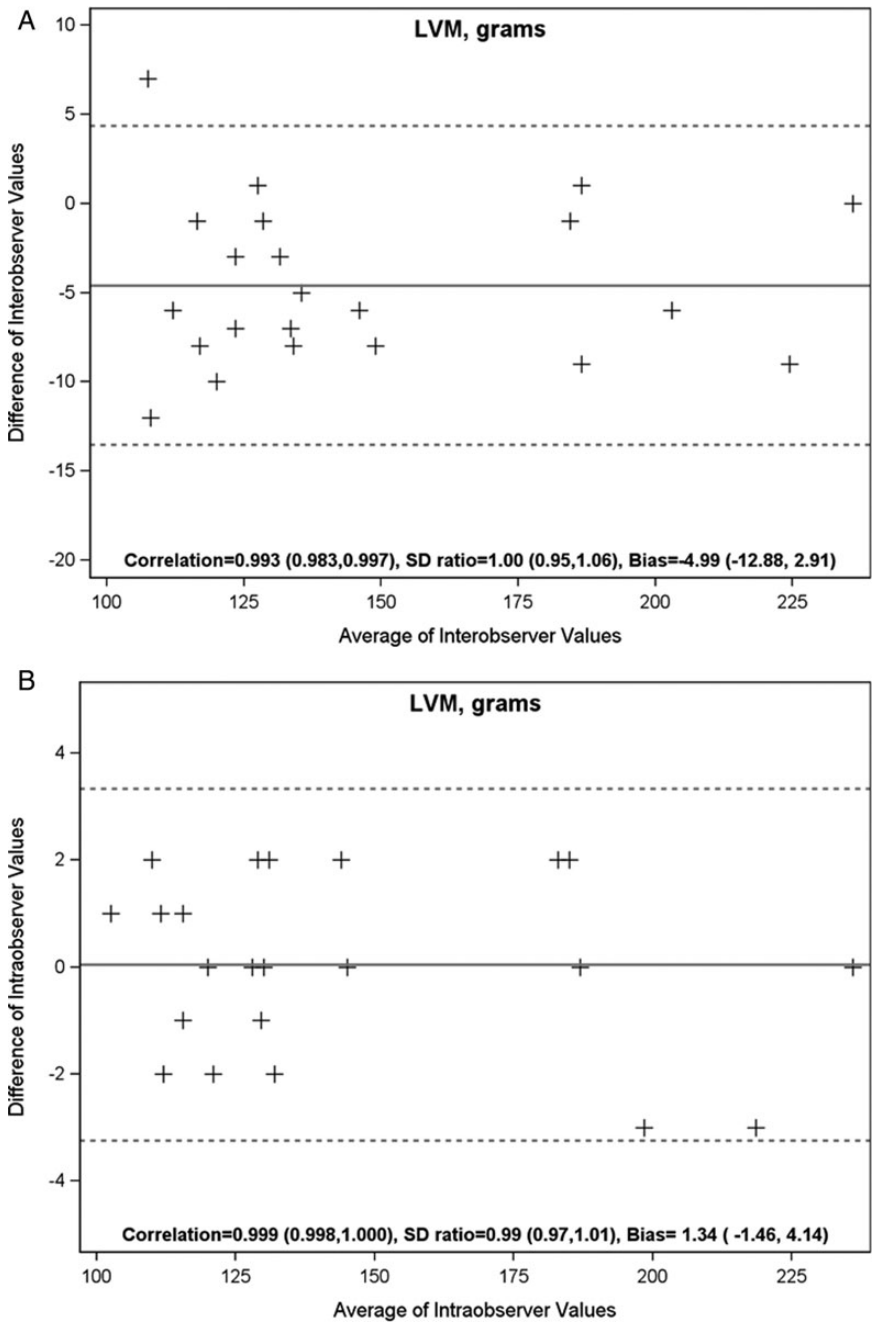

Figure 5: Variability of inter- and intra-observer measurements.

Relationship of LVM with myocardial ischaemia

In our study, LVMi was associated with SRS ≥ 1 and SSS ≥ 1 independent of cardiovascular risk factors and obstructive CAD, but not with SDS ≥ 1. Furthermore, LVM was associated only with SRS ≥ 1 when patients with fixed defects were excluded from the analysis. This observation confirmed that LVMi was associated only with SSS ≥ 1 when patients with infarcts were included. LV hypertrophy is an adaptive response during post-infarction remodelling that offsets increased load, attenuates progressive dilatation, and stabilizes contractile function.[23] The adaptive response indicated that replacement or scarring fibrosis corresponded to the replacement of myocyte after cell damage or necrosis by fibrosis.[23,24] Interstitial fibrosis from chronic exposure to cardiovascular risk such as hypertension and diabetes ultimately leads to replacement fibrosis in the later stages of disease.[24,25]

The diagnostic accuracy of MPD for detecting CAD in the presence of LV hypertrophy remains unclear due to myocardial microvascular disease.[26] Salcedo *et al.*[27] demonstrated that CAD and

LVMi are independent predictors of myocardial ischaemia in patients without MI. Furthermore, LV hypertrophy increases the incidence of perfusion defects in hypertensive patients without CAD.[28,29] LV remodelling is an independent predictor of the coronary flow reserve in hypertensive patients.[30] However, our findings do not associate LVMi with myocardial ischaemia in all patients. We report that, only among patients with previous MI, LVMi is independently associated with myocardial ischaemia. Various factors affect myocardial ischaemia through an increase in myocyte mass: increased myocardial oxygen demand, increased coronary vascular and minimal vascular resistance, decreased myocardial oxygen supply dependent on coronary blood flow, myocardial blood flow, and coronary flow reserve.[31] Coronary microvascular dysfunction may contribute to myocardial ischaemia, analogous to patients with hypertrophic cardiomyopathy.[32] LVM with ischaemia—as shown in hypertensive cardiomyopathy—contributes to increased myocardial fibrosis.[24] One of the mechanisms is associated with cardiac anti-angiogenesis. Sano *et al.* investigated whether pressure overload induced an accumulation of p53 that inhibited hypoxia-inducible factor-1 activity. The inhibition of angiogenesis prevents the development of cardiac hypertrophy and reduces the myocardial oxygen supply.[33] LVMi was associated with NormTAV as a total plaque volume index with MI. These results potentially indicate that myocardial microvascular disease occurred on the basis of these mechanisms.

Study limitations

Total coronary atheroma assessment was limited to non-stented segments, and we excluded coronary artery <1.5 mm diameter because even modern CT technologies have limited spatial resolution when compared with intravascular ultrasound (IVUS). We also acknowledge that total atheroma volume measured with CTA was not validated with either IVUS or optical coherence tomography as a reference standard. Validation of quantitative coronary atheroma software, however, has been reported.[14] The correlation of quantitative atheroma analysis was high.

Conclusion

LVM was independently associated with coronary artery atherosclerosis and MI.

Supplementary data

Supplementary data are available at *European Heart Journal – Cardiovascular Imaging* online.

Conflict of interest: none declared.

Funding

The sponsor of the CORE320 study, Toshiba Medical Systems Corporation, was not involved during any stage of the planning, design, data acquisition, data analysis, or manuscript preparation of this study.

References

1. Armstrong AC, Gidding S, Gjesdal O, Wu C, Bluemke DA, Lima JA. LV mass assessed by echocardiography and CMR, cardiovascular outcomes, and medical practice. *JACC Cardiovasc Imaging* 2012;**5**:837–48.
2. Bluemke DA, Kronmal RA, Lima JAC, Liu K, Olson J, Burke GL *et al.* The relationship of left ventricular mass and geometry to incident cardiovascular events. The MESA (Multi-Ethnic Study of Atherosclerosis) Study. *J Am Coll Cardiol* 2008;**52**:2148–55.
3. Levy D, Garrison RJ, Savage DD, Kannel WB, Castelli WP. Left ventricular mass and incidence of coronary heart disease in an elderly cohort. The Framingham Heart Study. *Ann Intern Med* 1989;**110**:101–7.
4. Lang RM, Bierig M, Devereux RB, Flachskampf FA, Foster E, Pellikka PA *et al.* Recommendations for chamber quantification: a report from the American Society of Echocardiography's Guidelines and Standards Committee and the Chamber Quantification Writing Group, developed in conjunction with the European Association of Echocardiography, a branch of the European Society of Cardiology. *J Am Soc Echocardiogr* 2005;**18**:1440–63.
5. Ghali JK, Liao YL, Cooper RS. Influence of left ventricular geometric patterns on prognosis in patients with or without coronary artery disease. *J Am Coll Cardiol* 1998;**31**:1635–40.
6. Rybicki FJ, Otero HJ, Steigner ML, Vorobiof G, Nallamshetty L, Mitsouras D *et al.* Initial evaluation of coronary images from 320-detector row computed tomography. *Int J Cardiovasc Imaging* 2008;**24**:535–46.
7. Lin FY, Devereux RB, Roman MJ, Meng J, Jow VM, Jacobs A *et al.* Cardiac chamber volumes, function, and mass as determined by 64-multidetector row computed tomography: mean values among healthy adults free of hypertension and obesity. *JACC Cardiovasc Imaging* 2008;**1**:782–6.
8. Greupner J, Zimmermann E, Grohmann A, Dubel HP, Althoff TF, Borges AC *et al.* Head-to-head comparison of left ventricular function assessment with 64-row computed tomography, biplane left cineventriculography, and both 2- and 3-dimensional transthoracic echocardiography: comparison with magnetic resonance imaging as the reference standard. *J Am Coll Cardiol* 2012;**59**:1897–907.
9. Truong QA, Toepker M, Mahabadi AA, Bamberg F, Rogers IS, Blankstein R *et al.* Relation of left ventricular mass and concentric remodeling to extent of coronary artery disease by computed tomography in patients without left ventricular hypertrophy: ROMICAT study. *J Hypertens* 2009;**27**:2472–82.
10. Heupler S, Lauer M, Williams MJ, Shan K, Marwick TH. Increased left ventricular cavity size, not wall thickness, potentiates myocardial ischemia. *Am Heart J* 1997;**133**:691–7.
11. Vavere AL, Simon GG, George RT, Rochitte CE, Arai AE, Miller JM *et al.* Diagnostic performance of combined noninvasive coronary angiography and myocardial perfusion imaging using 320 row detector computed tomography: design and implementation of the CORE320 multicenter, multinational diagnostic study. *J Cardiovasc Comput Tomogr* 2011;**5**:370–81.
12. Rochitte CE, George RT, Chen MY, Arbab-Zadeh A, Dewey M, Miller JM *et al.* Computed tomography angiography and perfusion to assess coronary artery stenosis causing perfusion defects by single photon emission computed tomography: the CORE320 study. *Eur Heart J* 2013;**35**:1120–30.
13. George RT, Arbab-Zadeh A, Cerci RJ, Vavere AL, Kitagawa K, Dewey M *et al.* Diagnostic performance of combined noninvasive coronary angiography and myocardial perfusion imaging using 320-MDCT: the CT angiography and perfusion methods of the CORE320 multicenter multinational diagnostic study. *AJR Am J Roentgenol* 2011;**197**:829–37.
14. de Graaf MA, Broersen A, Kitslaar PH, Roos CJ, Dijkstra J, Lelieveldt BP *et al.* Automatic quantification and characterization of coronary atherosclerosis with computed tomography coronary angiography: cross-correlation with intravascular ultrasound virtual histology. *Int J Cardiovasc Imaging* 2013;**29**:1177–90.
15. Papadopoulou SL, Garcia-Garcia HM, Rossi A, Girasis C, Dharampal AS, Kitslaar PH *et al.* Reproducibility of computed tomography angiography data analysis using semi-automated plaque quantification software: implications for the design of longitudinal studies. *Int J Cardiovasc Imaging* 2013;**29**:1095–104.
16. Papadopoulou SL, Neefjes LA, Garcia-Garcia HM, Flu WJ, Rossi A, Dharampal AS *et al.* Natural history of coronary atherosclerosis by multislice computed tomography. *JACC Cardiovasc Imaging* 2012;**5**(Suppl 3):S28–37.
17. Miller JM, Rochitte CE, Dewey M, Arbab-Zadeh A, Niinuma H, Gottlieb I *et al.* Diagnostic performance of coronary angiography by 64-row CT. *N Engl J Med* 2008;**359**:2324–36.
18. Cerci RJ, Arbab-Zadeh A, George RT, Miller JM, Vavere AL, Mehra V *et al.* Aligning coronary anatomy and myocardial perfusion territories: an algorithm for the CORE320 multicenter study. *Circ Cardiovasc Imaging* 2012;**5**:587–95.
19. Hachamovitch R, Nutter B, Hlatky MA, Shaw LJ, Ridner ML, Dorbala S *et al.* Patient management after noninvasive cardiac imaging results from SPARC (Study of Myocardial Perfusion and Coronary Anatomy Imaging Roles in Coronary Artery Disease). *J Am Coll Cardiol* 2012;**59**:462–74.
20. Cooper RS, Simmons BE, Castaner A, Santhanam V, Ghali J, Mar M. Left ventricular hypertrophy is associated with worse survival independent of ventricular function and number of coronary arteries severely narrowed. *Am J Cardiol* 1990;**65**:441–5.
21. Lin FY, Nicolo D, Devereux RB, Labounty TM, Dunning A, Gomez M *et al.* Nonobstructive coronary artery disease as detected by 64-detector row cardiac computed

tomographic angiography is associated with increased left ventricular mass. *J Cardiovasc Comput Tomogr* 2011;**5**:158–64.
22. Lieb W, Xanthakis V, Sullivan LM, Aragam J, Pencina MJ, Larson MG *et al.* Longitudinal tracking of left ventricular mass over the adult life course: clinical correlates of short- and long-term change in the Framingham offspring study. *Circulation* 2009;**119**:3085–92.
23. St. John Sutton MG, Sharpe N. Left ventricular remodeling after myocardial infarction: pathophysiology and therapy. *Circulation* 2000;**101**:2981–8.
24. Mewton N, Liu CY, Croisille P, Bluemke D, Lima JA. Assessment of myocardial fibrosis with cardiovascular magnetic resonance. *J Am Coll Cardiol* 2011;**57**:891–903.
25. Weber KT, Brilla CG. Pathological hypertrophy and cardiac interstitium: fibrosis and renin-angiotensin-aldosterone system. *Circulation* 1991;**83**:1849–65.
26. Chin D, Battistoni A, Tocci G, Passerini J, Parati G, Volpe M. Non-invasive diagnostic testing for coronary artery disease in the hypertensive patient: potential advantages of a risk estimation-based algorithm. *Am J Hypertens* 2012;**25**:1226–35.
27. Salcedo EE, Marwick TH, Korzick DH, Goormastic M, Go RT. Left ventricular hypertrophy sensitizes the myocardium to the development of ischaemia. *Eur Heart J* 1990; **11**(Suppl G):72–8.
28. Houghton JL, Frank MJ, Carr AA, von Dohlen TW, Prisant LM. Relation among impaired coronary flow reserve, left ventricular hypertrophy and thallium perfusion defects in hypertensive patients without obstructive coronary artery disease. *J Am Coll Cardiol* 1990;**15**:43–51.
29. Pringle SD, Dunn FG, Tweddel AC, Martin W, Macfarlane PW, McKillop JH *et al.* Symptomatic and silent myocardial ischaemia in hypertensive patients with left ventricular hypertrophy. *Br Heart J* 1992;**67**:377–82.
30. Schäfer S, Kelm M, Mingers S, Strauer BE. Left ventricular remodeling impairs coronary flow reserve in hypertensive patients. *J Hypertens* 2002;**20**:1431–7.
31. Camici PG, Olivotto I, Rimoldi OE. The coronary circulation and blood flow in left ventricular hypertrophy. *J Mol Cell Cardiol* 2012;**52**:857–64.
32. Timmer SAJ, Knaapen P. Coronary microvascular function, myocardial metabolism, and energetics in hypertrophic cardiomyopathy: Insights from positron emission tomography. *Eur Heart J Cardiovasc Imaging* 2013;**14**:95–101.
33. Sano M, Minamino T, Toko H, Miyauchi H, Orimo M, Qin Y *et al.* p53-induced inhibition of Hif-1 causes cardiac dysfunction during pressure overload. *Nature* 2007;**446**:444–8.

IMAGE FOCUS

doi:10.1093/ehjci/jeu189
Online publish-ahead-of-print 21 October 2014

Coronary steal phenomenon from a coronary artery to left ventricular fistula

Nikita V. Carvalho*, Disha A. Desouza, Kavit A. Desouza, and Nirat Beohar

Interventional Cardiology, Columbia University Division of Cardiology at Mount Sinai Medical Center, 4300 Alton Road, Miami Beach, FL 33140, USA

* Corresponding author. Tel: +1 305 674 2000; Email: nikitavc88@gmail.com

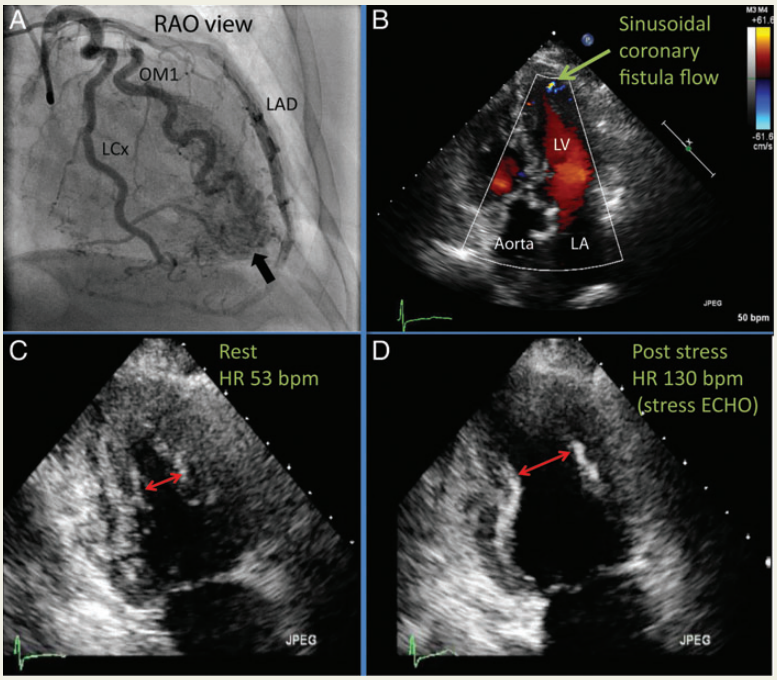

An 83-year-old female with well-controlled hypertension presented with gradually worsening dyspnoea on exertion. An exercise stress echocardiogram showed left ventricular hypertrophy with high-risk features for ischaemia at peak stress. Her left ventricular (LV) ejection fraction (LVEF) deteriorated from 65% at rest to 40% post-exercise, despite a submaximal stress test, stopped prematurely due to severe dyspnoea. She developed hypokinesis of the anterior septum, lateral and anterior walls during post-stress echocardiographic imaging as seen on the apical two-chamber view in the post-stress image (*Panel D*), compared with the resting image (*Panel C*) during end-systole (also see Supplementary data online, *Videos S1* and *S2*). A subsequent left heart catheterization revealed a large calibre-dominant left coronary artery, with a large coronary artery to LV fistula from the left circumflex (LCx) and obtuse marginal (OM1) arteries, emptying into the LV cavity via a sinusoidal network (arrow in *Panel A* and Supplementary data online, *Videos S3–S5*). There was no significant coronary artery stenosis, with a normal LVEF on left ventriculography and an elevated LV end-diastolic pressure of 27 mmHg. The fistula was also evident on transthoracic echocardiogram (*Panel B* and Supplementary data online, *Video S6*) as multiple turbulent jets in the LV myocardium draining towards the LV cavity during diastole. Hence her stress-induced ischaemia was likely due to coronary artery steal phenomenon from her coronary artery fistula.

AP, anterior–posterior; RAO, right anterior oblique; LAD, left anterior descending artery.

Supplementary data are available at *European Heart Journal – Cardiovascular* Imaging online.